Controlling the optical response of 2d matter in standing waves

Eric Plum[,1], Kevin F. MacDonald[*,1], Xu Fang[2], Daniele Faccio[3], Nikolay I. Zheludev[*,1,4]*

[1]Optoelectronics Research Centre and Centre for Photonic Metamaterials, University of Southampton, Highfield, Southampton, SO17 1BJ, UK;

[2]Electronics and Computer Science, University of Southampton, Highfield, Southampton, SO17 1BJ, UK;

[3]School of Engineering and Physical Sciences, SUPA, Heriot-Watt University, Edinburgh EH14 4AS, UK;

[4]Centre for Disruptive Photonic Technologies, School of Physical and Mathematical Sciences and The Photonics Institute, Nanyang Technological University, Singapore 637371

E-mail: erp@orc.soton.ac.uk; kfm@orc.soton.ac.uk; niz@orc.soton.ac.uk

Abstract: There is a major development in photonic technology unfolding that promises to change optical data processing paradigms, spectroscopy and nonlinear / quantum optics. This new direction has its roots in plasmonics, metamaterials and coherent optics: It has been discovered in recent years that the optical properties of thin-film media can, if the film is much thinner that the wavelength, manifest differently in travelling wave and standing wave light fields. In the latter case, 'coherent control' of the energy exchange between incident and scattered waves leads to a plethora of new technological opportunities including single photon gates, 100 THz all-optical modulators, a ground-breaking spectroscopy technique that can distinguish different multipole contributions to absorption and quantum optical devices. We provide an overview of the rapidly growing body of work on the optics of planar (ultrathin) media and metamaterials in coherent light fields.

Keywords: standing wave, metamaterial, metasurface, plasmonics, all-optical, coherent perfect absorption

Introduction

Coherent control is a well-understood concept in quantum mechanics[1], where it is used to direct dynamic processes with light by engaging quantum interference phenomena. Coherent control concepts have also been employed to manipulate processes such as the direction of electron motion in semiconductors[2]; breaking of chemical bonds[3]; the absorption[4-8] and localization[9-13] of light in cavities and at surfaces; transmission of light by metal-dielectric stacks[14-15]; light modulation in waveguides[16-18]; nonlinear optical phenomena in periodic structures[19] and nanoparticles[20]; polarization rotation in Faraday media[21-22]; optical effects in optomechanical systems[23-24]; the excitation and propagation of surface plasmon polaritons at metal/dielectric interfaces[25-27], as well as the absorption of acoustic waves[28-29], see Fig. 1.

The paradigm is now being harnessed to manipulate the manifestation of all kinds of light-matter interactions with exquisite precision in planar photonic (meta)materials, where one can uniquely engineer combinations of reflection, transmission, absorption and polarization properties that are not possible in naturally occurring media. We begin with a theoretical description of such interactions of coherent light with planar materials, followed by a review of the resulting opportunities from all-optical modulation of intensity, propagation direction and polarization of light to applications in data and image processing as well as quantum technologies.

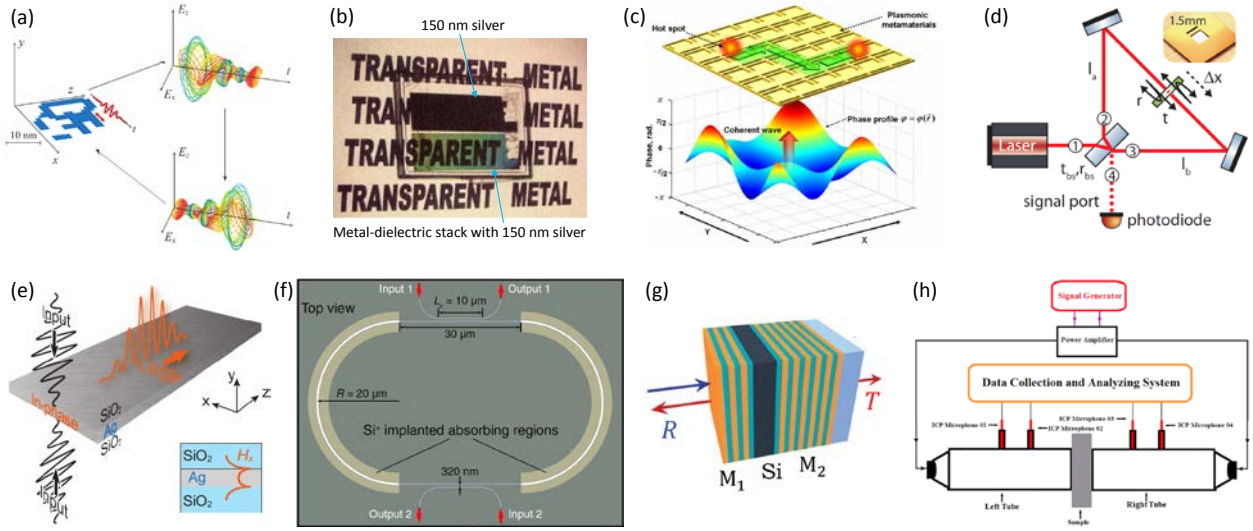

Fig. 1: Coherent control of various phenomana across many disciplines. (a) Nanosecond-femtosecond spatiotemporal field localization in plasmonic systems by time reversal[10]. (b) Transparent metal-dielectric stacks[15]. (c) Nanoscale light localization in metamaterials[11]. (d) Quantum opto-mechanics based on destructive interference on a nanomembrane oscillator[23]. (e) Selective excitation of long-range surface plasmon polaritons[27]. (f) Silicon photonic modulator based on coherent perfect absorption[18]. (g) Multi-band coherent perfect absorption in silicon controlled by aperiodic dielectric mirrors M[8]. (h) Coherent perfect absorption of sound[29].

Interaction of coherent light with 2D matter

Consider a layer of absorbing material illuminated at normal incidence by a pair of counter-propagating, collinearly polarized coherent light waves: The incident fields E_α and E_β represent input signals; the transmitted and reflected waves (fields E_γ and E_δ) propagating away from the film on either side constitute output signals (Fig. 2). Assuming a purely linear, dipolar response with no change in the polarization state of light, the input and output fields are related by a complex scattering matrix [30] $\boldsymbol{S}$:

$$\begin{bmatrix} E_\delta \\ E_\gamma \end{bmatrix} = \begin{bmatrix} \boldsymbol{S_{11}} & \boldsymbol{S_{12}} \\ \boldsymbol{S_{21}} & \boldsymbol{S_{22}} \end{bmatrix} \begin{bmatrix} E_\alpha \\ E_\beta \end{bmatrix} \qquad (1)$$

where $\boldsymbol{S_{11}}$ and $\boldsymbol{S_{21}}$ are respectively the reflection and transmission coefficients for light incident on the medium from side 1; $\boldsymbol{S_{22}}$ and $\boldsymbol{S_{12}}$ being the same for incidence on side 2. In the absence of any magneto-optical effects, reciprocity dictates that $\boldsymbol{S_{12}} = \boldsymbol{S_{21}}$, so three independent parameters are necessary to describe the optical properties of such a device.

An effective nonlinearity is derived, in this simple four-port device geometry, from the coherent nature of beam interactions that are described by matrix (1): The linearity of the film's properties implies that if both input signals are scaled by the same factor η, both of the resulting output signals must also scale by η. But there is absolutely nothing to dictate any proportional scaling of one, other or both outputs when only one of the inputs is changed. Thus, the relationship between a given input port and a given output port in a coherent four-port device based upon a linear medium can, counterintuitively, be nonlinear. This nonlinear response results from the linear interaction of coherent light waves on a linear material.

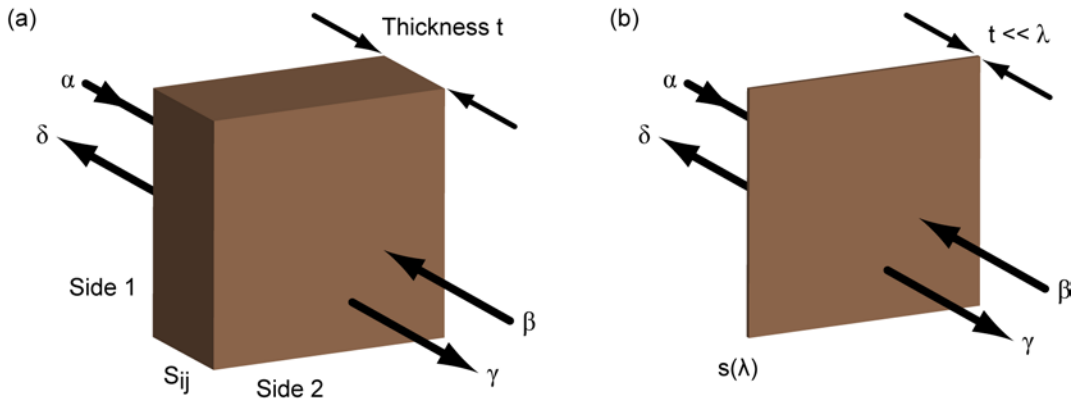

Fig. 2: Generic four-port coherent control device. (a) A medium, with optical properties described by a complex scattering matrix S_{ij} containing three independent parameters, is illuminated by counter-propagating coherent input light waves α and β; waves γ and δ are the device outputs. (b) In the limit of substantially subwavelength thickness, the medium can be described by a single complex scattering coefficient $s(\lambda)$.

In principle, the effective nonlinearity of a four-port device can be observed using any interaction medium: Equation (1) places no constraints on the thickness of the film, which may be single- or multi-layered, and each layer may be homogenous or nanostructured (though only at the subwavelength scale to exclude diffraction effects); the only requirement is that the incident beams must be coherent.

Nevertheless, film thickness is a crucial factor in many cases, including for achieving high contrast control over absorption of light and associated all-optical information processing and spectroscopy applications. Here, contrast from complete transparency to perfect absorption may be achieved based on the very different strength of light-matter interaction of a thin film placed at a node or anti-node of a standing wave. The challenge therefore lies in achieving the requisite balance among reflection, transmission and absorption in a medium of sufficiently subwavelength optical thickness to harness this contrast. In the optical part of the spectrum this is more challenging than one might imagine because, in the limit of very small but nonetheless finite thickness nature offers a surprisingly limited palette of properties – most conventional materials are either highly transparent or highly reflecting; large single-beam, single-pass absorption is almost impossible to achieve with normal materials.

Planar metamaterials or metasurfaces though - man-made media structured on the subwavelength scale - provide unprecedented freedom to engineer the balance among resonant absorption, reflection and transmission almost at will in ultrathin metal, dielectric and semiconductor films. Nanostructuring of thin film materials introduces optical resonances with a strength and spectral position that is controlled by the geometry and size of the nanostructure, allowing strong light-matter interactions to be achieved in films of nanoscale thickness and resulting in the above-mentioned freedom to engineer metamaterial optical properties, which uniquely enable four-port optical devices to be configured to deliver a broad range of functionalities with high optical contrast.

Consider now a target film of sufficient thinness that retardation effects across it can be ignored, i.e. we may consider each constituent molecule to be exposed to the same electric field - the combined field $E_\alpha + E_\beta$ of the incident waves. Absorbed energy will be re-radiated equally in the forward and backward directions with an efficiency dependent on the excitation wavelength λ and proportional to the driving field, i.e., to $s(\lambda)(E_\alpha + E_\beta)$, where $s(\lambda)$ is a complex wavelength-dependent scattering coefficient for the film under single-beam illumination[31]. The magnitude and phase of $s(\lambda)$ respectively correspond to the relative amplitude of the re-radiated field and to the phase lag between re-radiated and driving fields. $s(\lambda)$ may include losses and thereby excludes any assumption of equality between the combined incident and combined output beam intensities. Requirements of field continuity then dictate the following *exact* scattering matrix expression relating input and output fields for a coherent four-port device based upon a *vanishingly* thin film (Fig. 2b):

$$\begin{bmatrix} E_\delta \\ E_\gamma \end{bmatrix} = \begin{bmatrix} s(\lambda) & s(\lambda)+1 \\ s(\lambda)+1 & s(\lambda) \end{bmatrix} \begin{bmatrix} E_\alpha \\ E_\beta \end{bmatrix} \qquad (2)$$

As it must, for single-beam illumination – with one or other of the inputs set to zero, this expression reduces to stipulate that the reflected field is equal to the re-radiated field and the transmitted field to the sum of incident and re-radiated fields.

In cases where the contribution from interference among multiply reflected/transmitted beams is small, Eq. (2) can serve as a good approximation to the analytical expression of Eq. (1) for realistic (i.e., finite as opposed to infinitely thin) materials. This greatly simplifies the consideration and analysis of four-port coherent device functionalities by reducing the number of free parameters required to describe the system from three ($\boldsymbol{S_{ij}}$) to one, in the form of $s(\lambda)$.

At the node of a standing wave formed by counter-propagating coherent incident beams, $E_\alpha = -E_\beta$. With an ultrathin medium positioned at the node, E_γ will thus always be equal to E_α, and E_δ to E_β, regardless to the value of the film's scattering parameter $s(\lambda)$. This is the "coherent perfect transmission" regime - a situation in which there is no light-matter interaction because the film is located at a point where the net electric field is zero. We note that coherent perfect transparency of weakly absorbing films has long been exploited for laser mode selection[32-37]. At an anti-node of the standing wave, on the other hand, $E_\alpha = E_\beta$. Here, both E_γ and E_δ can be reduced to zero if $s(\lambda) = -0.5$, whereby the film exhibits the maximum possible level of zero-thickness single-beam absorption [38-39], namely 50%. This is the regime of "coherent perfect absorption". It is interesting to note here that while perfect transparency requires an absorber of substantially subwavelength thickness [40], the phenomenon of coherent perfect absorption does not. Indeed, the latter has been demonstrated in a variety of optically thick media and spectral domains [5, 8, 41-43]. Any ultrathin film will manifest coherent perfect transparency at a standing wave node, but it is only in special cases such as metamaterial nanostructuring or use of multi-layer graphene that one may engineer a level of single-beam absorption in a film such that it will also manifest perfect coherent absorption at an anti-node. These node/anti-node limiting cases of standing wave light-matter interactions can be understood intuitively, but in what follows we also consider intermediate values of the incident waves' mutual phase $\theta = arg\ E_\alpha - arg\ E_\beta$ in the plane of ultrathin target media and their relevance to signal processing functions.

The effective optical nonlinearity of coherent four-port devices, i.e. the nonlinear relationship between selected input and output port intensities, which again should not be confused with the purely linear nature of the thin-film medium's optical response, is readily illustrated in the limit of deeply subwavelength interaction media, i.e. on the basis of Eq. (2) as opposed to Eq. (1). Consider the intensity (defined as $I = EE^*$) of output γ:

$$I_\gamma = |1 + s(\lambda)|^2 I_\alpha + |s(\lambda)|^2 I_\beta + 2Re\{(1 + s(\lambda))s^*(\lambda)E_\alpha E_\beta^*\} \qquad (3)$$

Clearly, if one of the two input signals is removed, the system reverts to a truly linear single-beam mode of operation wherein output signal intensities are strictly proportional to that of the remaining input. And, if input intensities I_α and I_β are increased or decreased in proportion, there will be a correspondingly proportional increase or decrease in I_γ. However, if I_α remains fixed and only I_β changes, then I_γ will respond in a nonlinear fashion as illustrated in Fig. 3 for the case where $s(\lambda) = -0.5$ and $I_\alpha = 1$: here the dependence of I_γ on I_β is not only nonlinear but also nonmonotonic for $\theta < 90°$.

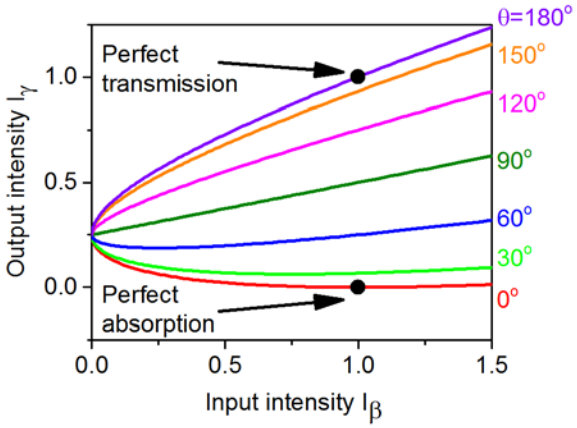

Fig. 3: Nonlinear response function of a generic four-port coherent device. Dependence of output intensity I_γ on input intensity I_β for a fixed input intensity $I_\alpha = 1$, for a selection of mutual phase settings θ between E_α and E_β (as labelled) in the plane of a vanishingly thin absorber with a scattering parameter $s(\lambda) = -0.5$.

Light propagating in a conventional nonlinear (bulk) medium experiences harmonic distortion, which can lead ultimately to optical instability and multi-stability. The nonlinear character of a four-port coherent device however, is different: it is based upon the re-distribution of energy among ports and does not cause harmonic distortion; it is underpinned only by linear interference effects and as such is of course strictly compliant with energy conservation; a variety of functionalities are enabled by the fact that the level of absorption in such devices is not fixed, but is instead strongly dependent on the mutual intensity and phase of input beams.

It is apparent from the above analysis that generically an effective nonlinearity may be obtained using any homogenous ultrathin film including, for example, a 50:50 beamsplitter. However, in the absence of absorption there can be no coherent modulation of absorption (the maximum achievable level of coherent absorption being twice the film's single beam absorption level). The range of achievable input-output functions is then constrained effectively to those of a conventional interferometer. In this context, photonic metamaterials are an enabling technology, providing access to an otherwise inaccessible range of ultrathin-film scattering coefficients $s(\lambda)$ at any desired wavelength by nanostructural design, and thereby to a wide range of nonlinear response functions applicable to all-optical signal processing functionalities.

Before addressing specific metamaterial designs and coherent four-port device functionalities based upon such structures, we shall consider the meaning of $s(\lambda)$ scattering coefficient values, with reference to a selection of more familiar materials in ultrathin film form, looking first at levels of single-beam illumination, single-pass absorption given by the expression

$$A = 1 - |s(\lambda)|^2 - |s(\lambda) + 1|^2 \qquad (4)$$

It should be emphasised that $s(\lambda)$ is purely a material parameter, it assumes nothing as to the mode of illumination (single-beam or coherent). Figure 4a however maps levels of single-beam absorption onto the complex $s(\lambda)$ parameter space.

The red circular line in Fig. 4 satisfies the condition $A = 0$, which is to say that it describes lossless media that neither absorb nor amplify incident light. It defines a boundary between absorbing materials ($A > 0$, inside the circle) and gain media ($A < 0$, outside the circle). At the central point of the circle $A = 0.5$, i.e. the maximum possible level of single-beam absorption permitted by field continuity constraints in a vanishingly thin film [38-39]. It corresponds to a material film with a scattering parameter $s(\lambda) = -0.5$.

A thin film of empty space (i.e vacuum) will obviously transmit 100% of incident light at any wavelength without changing its phase. It has a value $s(\lambda) = 0$ represented in the $s(\lambda)$ plane by a single point on the zero-loss contour as shown in Fig. 4. A thin film of perfect electric conductor (PEC), on the other hand, will reflect

100% of incident light at any wavelength with a π phase change. With a value $s(\lambda) = -1$ it is represented by a point diametrically opposite vacuum (or air) on the zero-loss line in $s(\lambda)$ space. Thin, ideally transparent glass films with a fixed refractive index of 1.5 also sit on the zero-loss contour, being represented over a given wavelength range (for a given thickness) by a line as opposed to a singular point – traces are plotted in Fig. 4b for glass films of 10 and 50 nm thicknesses for wavelengths from 750 to1050 nm. Gold thin films are again dispersive but highly reflective and weakly absorbing, so they appear in $s(\lambda)$ space as lines lying just inside the zero-loss contour. Indeed, in the zero-thickness limit, most naturally occurring homogenous materials have weakly dispersive $s(\lambda)$ coefficients close to the zero-loss contour.

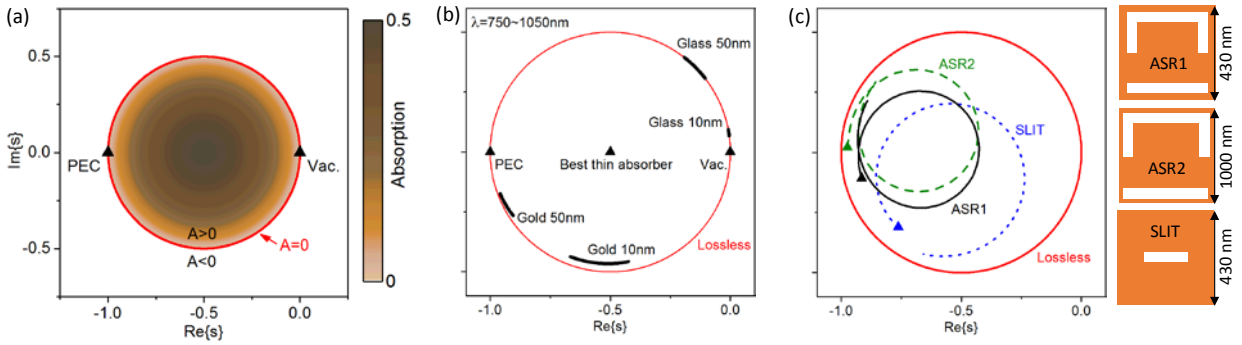

Fig. 4: The scattering coefficient $s(\lambda)$ of ultrathin films and associated properties. (a) Level of absorption A of a ultrathin film illuminated from only one side as a function of its scattering coefficinet s. (b) Scattering coefficients for homogenous thin film media in the 750 - 1050 nm wavelength range. (c) Scattering coefficients for selected periodic planar metamaterials indicated by their unit cells, modelled in COMSOL Multiphysics. The designs ASR1, ASR2 and SLIT consist of gold on silicon nitride with layer thicknesses of 50/30, 50/30, 30/30 nm and the scattering coefficients are plotted for wavelength ranges of 750-1050, 1250-1850 and 750-1050 nm, respectively, with a triangular marker indicating the shortest wavelength. Modelling assumed a Drude-Lorentz model for the properties of gold and a fixed refractive index of 2.0 for silicon nitride, with normal monochromatic plane-wave illumination linearly polarized with the electric field parallel to the common symmetry axis of the nanostructures.

In contrast, metamaterial nanostructures can provide access by design to the full parameter space. This is illustrated by Fig. 4c, showing the range of scatting coefficients accessible with several generic planar metamaterial nanostructures of sub-100nm thickness. These are arrays of asymmetric split ring (ASR) and slot apertures in a bilayer of gold and silicon nitride. ASR designs have been employed and optimized in numerous previous studies [44-45], including the first experimental demonstrations of coherent absorption modulation[40, 46]. The scattering coefficients of metamaterial ASR1 for wavelengths between 750 and 1050 nm describe a loop extending from the neighbourhood of the zero-loss contour, towards the centre of the $A > 0$ domain with 'ideal, zero-thickness absorber' characteristics at 870 nm wavelength, and back. This $s(\lambda)$ trace can be modified simply by adjusting the dimensions of the metamaterial structure: the ASR2 line for example represents a gold/silicon nitride metamaterial design with an absorption resonance centred at 1550 nm. And of course, the ASR is only one of an almost infinite number of possible designs – a third trace is presented in Fig. 4c for a metamaterial comprising an array of linear slots again in a gold film on silicon nitride. Thus, the great power of the metamaterial paradigm lies in its ability to provide otherwise impossible optical properties by nanostructural design.

Coherent absorption modulation

As explained above, the interference of coherent light beams on an ultrathin layer of material, much thinner than the wavelength of light, can selectively render the medium almost perfectly transparent or facilitate

near-perfect optical absorption, thus enabling THz bandwidth light-by-light modulation[47] without conventional optical nonlinearity and therefore at arbitrarily low intensity[48].

Coherent control of absorption in standing waves has long been exploited for laser mode selection, where a lossy thin film is placed within the laser cavity at a node of the desired mode to selectively absorb competing modes[32-37]. Also coherent perfect absorption in thick structures[8, 41] – sometimes referred to as time-reversed lasing[4-5, 42-43] – has been known for some time.

Dynamic coherent control of thin film absorption from coherent perfect transparency to coherent perfect absorption was first observed by Zhang et al.[40] for a 50-nm-thick gold film perforated with an ASR aperture array and supported by a glass substrate (Fig. 5a). By controlling the interference of red laser light on the metasurface, that was 13x thinner than the wavelength, absorption was modulated from about 5% to about 85%, which is close to the ideal contrast of 0% to 100% absorption that would correspond to an ideally thin film with a scattering coefficient *s*=-0.5. As illustrated by Fig. 5b, near perfect transparency of the metasurface absorber results from destructive interference of counterpropagating coherent laser beams on the metasurface. I.e. the absorber is placed at an electric field node of the standing wave formed by both laser beams and therefore the charges within the 2D material – that are confined to the metasurface plane – cannot be accelerated by the light field, resulting in negligible light-matter interaction. In contrast, if the metasurface is located at a position of constructive interference, i.e. an anti-node of the standing wave, charge acceleration and thus the light-matter interaction is enhanced resulting in nearly complete absorption of all incident light. Apart from photonic metasurfaces made from plasmonic materials[40], dielectrics[49] or graphene[50], coherent perfect absorption and transparency has also been predicted in multi-band microwave metamaterials[51] and heavily doped silicon thin films for terahertz waves[52] as well as observed in 9-nm-thick 30-layer graphene[53], which exhibits broadband 50% absorption when illuminated by a single beam of light. In particular, the electric tunability of layered or structured graphene absorbers offers the interesting opportunity of electric modulation of coherent absorption[50], see Fig. 5c.

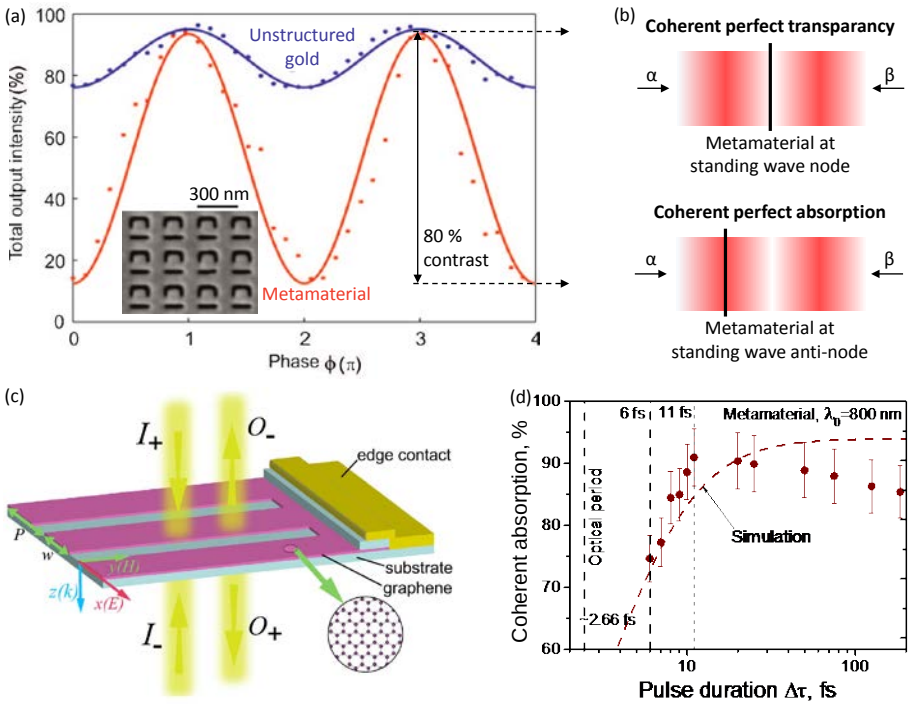

Fig. 5: Coherent absorption modulation in 2D matter. (a) First observation of coherent absorption and transparency for a planar metamaterial (50-nm-thick nanostructured gold supported by glass) illuminated by counterpropagating coherent laser beams at 633 nm wavelength linearly polarized parallel to the symmetry axis of the nanostructure[40]. (b) Schematic illustrating coherent perfect transparency and absorption resulting from destructive and constructive interference of incident electric fields α and β on a planar metamaterial. (c) Proposed scheme for electric control of mid-infrared coherent absorption in structured graphene[50]. (d) Coherent absorption at the standing wave anti-node measured with counterpropagating coherent femtosecond laser pulses for a plasmonic metamaterial consisting of a freestanding 60-nm-thick gold film perforated with an ASR aperture array of 320 nm period[47].

While optical nonlinearities suffer from a trade-off between speed and magnitude[54], Xu, Nalla and co-authors[46-47] have demonstrated that coherent absorption offers intensity-independent high contrast modulation of light with light even at femtosecond timescales. Fig. 5d shows coherent absorption measured in a plasmonic metasurface with femtosecond laser pulses. They show that absorption of about 90% can be achieved with laser pulses as short as 10 fs, corresponding to about 4 optical cycles and a bandwidth on the order of 100 THz.

The ability to control absorption of light with light without a nonlinear medium, with 100 THz bandwidth and without need for high intensities opens up a broad range of possibilities. As discussed later on, the resulting effective nonlinearity may be used to achieve various logical functions for ultrafast all-optical data processing, image recognition and analysis, as well as small signal amplification and coherence filtering.

Coherent control of refraction, polarization effects and nonlinear optical phenomena

While the ability to control absorption of light is very important, coherent interaction of light fields on planar materials can go much further. The superposition of coherent waves allows control over both the local electric and the local magnetic field from zero (destructive interference) to enhancement (constructive interference). By controlling the field in the plane of a 2D material, the interaction of coherent light fields may therefore be used to control the optical excitation of the material and thus the manifestation of any optical functionality the material may have. Opportunities include control over the relative efficiency of normal and anomalous refraction from phase-gradient metasurfaces, the manifestation of linear and circular birefringence and dichroism, and the efficiency of nonlinear optical responses with high contrast in ultrathin media, promising new functionalities for wavefront shaping and signal processing.

For example, Shi et al[55] suggested and studied coherent control of phase gradient metasurfaces, which are planar metamaterials consisting of “meta-molecules” that scatter with a spatially varying phase, resulting in transmission and reflection of light in anomalous directions[56]. Exploiting destructive interference of coherent light fields incident on a phase gradient metasurface from opposite sides, scattering and thus anomalous transmission and reflection may be turned off, whereas constructive interference yields anomalous transmission and reflection with enhanced efficiency, thus enabling dynamic redirection of light. An experimental realization was recently reported by Kita et al[57] using a gold phase gradient nanostructure with a partial back reflector that directs anomalous light emission preferentially to one side of the nanostructure, see Fig. 6a. Such all-optical beam deflection could have applications in signal routing and the concept could be extended to planar meta-lenses[58-59] and meta-holograms[60-61], that could also be coherently controlled.

Coherent control of polarization phenomena with very high contrast has been reported at microwave frequencies using anisotropic as well as 3D-chiral structures that are thin compared to the wavelength[62]. Coherent interaction of microwaves on an anisotropic metamaterial – resembling a wave plate – has allowed full control over the orientation of the plane of polarization. Arbitrary polarization rotation has also been achieved with an isotropic chiral thin film consisting of mutually twisted metal patterns in parallel planes spaced by few percent of a wavelength. Optical activity, that is the ability to rotate the polarization state of light (circular birefringence) and differential throughput for left and right-handed circular polarizations (circular dichroism), is usually observed in such 3D-chiral structures, i.e. structures that cannot be superimposed with their mirror image. While 3D-chiral structures can be very thin, they cannot be planar, however, optical activity does not require chiral materials. Instead, optical activity may also be observed if the mirror-symmetry of the experimental arrangement is broken by the illumination direction. Such so-called extrinsic 3D chirality leads to very large optical activity in planar metamaterials lacking rotational symmetry[63] and can also be coherently controlled. Coherent interaction of microwaves on an array of asymmetrically split metallic rings has allowed almost complete control over the ellipticity of electromagnetic waves from right-handed to left-handed circular polarization[64]. Fig. 6b illustrates the first demonstration of such polarization control in the visible part of the spectrum[65]. Constructive (or destructive) interference at oblique incidence is achieved by illuminating both sides of the metamaterial by coherent waves incident in the same plane with the same incidence angle on the same side of the surface normal as shown. This way, the phase difference between the incident waves is constant across the metamaterial. The metamaterial is an asymmetric split ring aperture array in a gold film with about 300 nm period and oblique incidence yields an extrinsically chiral experimental arrangement (except when the structure’s line of symmetry coincides with the plane of incidence). The manifestation of the resulting optical activity is then controlled by the phase difference of the

incident waves. For constructive interference of the incident electric fields significant circular dichroism (as well as circular birefringence) is observed, which increases with increasing angle of incidence. In contrast, destructive interference renders the nanostructure essentially transparent causing all polarization effects to vanish.

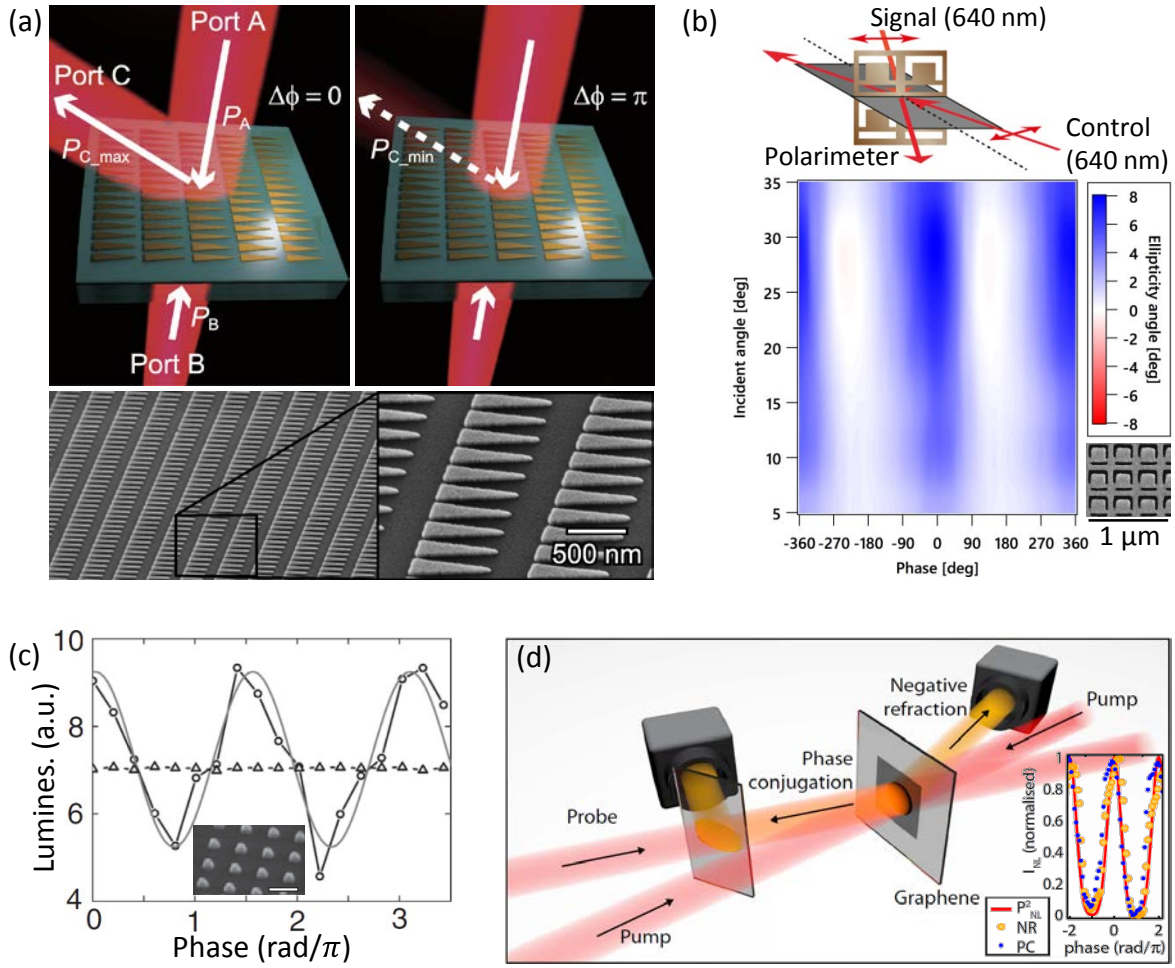

Fig. 6: Coherent control of anomalous reflection, polarization effects and nonlinear phenomena in the optical part of the spectrum. (a) Constructive interference ($\Delta\phi=0$) of incident waves A and B on a phase gradient metasurface leads to efficient anomalous reflection, while the anomalous beam vanishes almost completely in case of destructive interference ($\Delta\phi=\pi$)[57]. (b) Manifestation of optical activity of a metasurface controlled by constructive interference (phase 0) and destructive interference (phase ±180°) of 640 nm wavelength signal and control beams illuminating the nanostructure[65]. (c) Photoluminescence of dye molecules on aluminium nanopyramids (300 nm scale bar) as a function of the phase difference between coherent (circles) and incoherent (triangles) counterpropagating pump beams[66]. (d) Nonlinear response of 30-layer graphene controlled by constructive (phase 0) and destructive (phase π) interference of counterpropagating coherent pump beams on the nonlinear thin film at 780 nm wavelength. Time-averaged nonlinear polarization P^2_{NL} as well as negatively refracted (NR) and phase-conjugated (PC) beam amplitudes are shown[67].

Coherent interaction of light with light on thin films can also be exploited to control phenomena that change the wavelength of light. For example, Pirruccio et al reported that photoluminescence may be enhanced or suppressed through constructive interference of pump light on a luminescent thin film[68] or plasmonic nanostructures coupled to a luminescent material[66] (Fig. 6c), providing a route to phase-modulated light sources.

Not only linear, but also nonlinear phenomena can be controlled by two coherent beams of light. This has been explored by Rao et al[67] who studied nonlinear four-wave mixing in 30-layer graphene, which is about 9 nm thick, at a wavelength of 780 nm. By controlling the interference of two counterpropagating coherent pump beams on the thin graphene film (or one pump beam and its reflection on a mirror), the authors were

able to control the nonlinear polarization in the graphene film and thus various associated nonlinear phenomena including phase conjugation and negative refraction effects, see Fig. 6d.

Coherent excitation-selective spectroscopy

Important differences between interaction of light and matter in travelling and standing waves have previously been noted in the context of cavity ringdown spectroscopy[69-70] (Fig. 7a), where different levels of absorption were observed for thin samples positioned at a node or anti-node of a standing wave formed within a cavity. The importance of standing waves becomes clear when considering that plane traveling waves propagating in an isotropic medium (e.g. air) can be fully characterized by intensity, degree of polarization, ellipticity and polarization azimuth. They always have orthogonal electric and magnetic fields that are proportional to each other and these inseparable electric and magnetic fields make optical effects that depend on either electric or magnetic field difficult to distinguish. In contrast, standing waves, formed by counter-propagating coherent waves, offer additional degrees of freedom that allow probing of materials of substantially subwavelength thickness in ways that are not possible with travelling plane waves. For example, it has been predicted that non-radiating anapoles, formed by destructive interference of electric and toroidal dipoles, can be excited in this way[71].

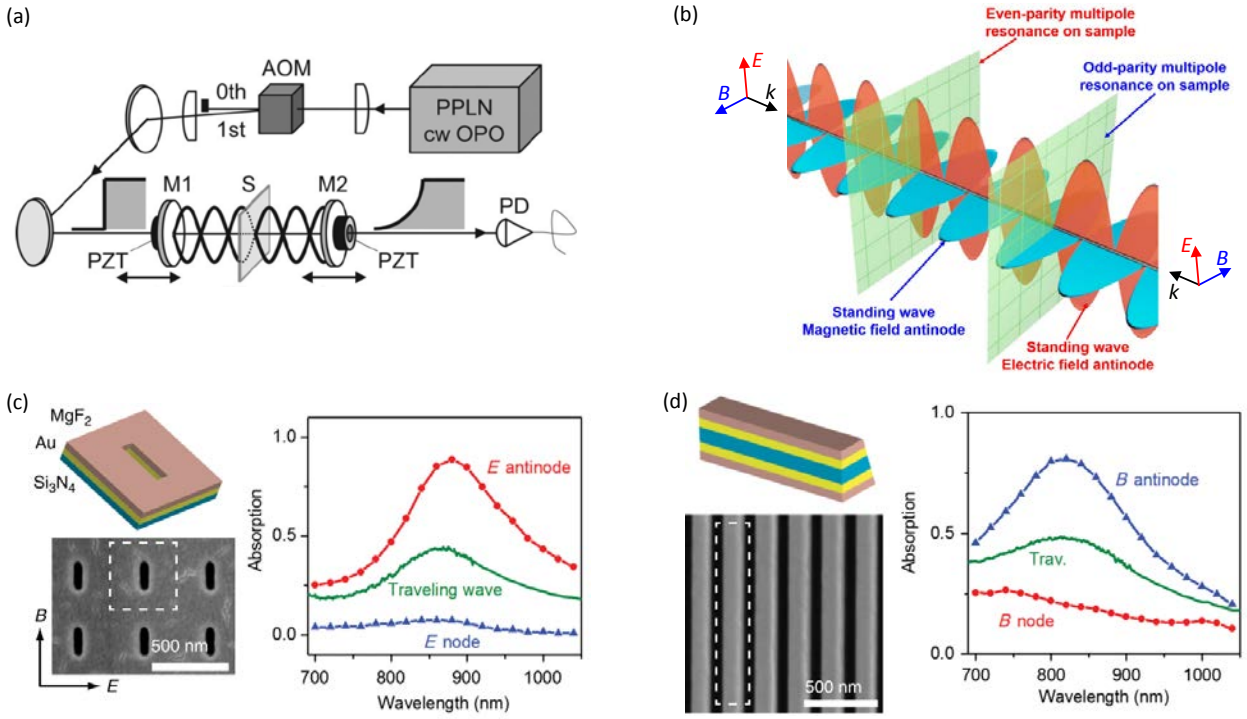

Fig. 7: Coherent spectroscopy in standing waves. (a) A schematic setup for photon-trap spectroscopy, a generalized form of cavity ringdown spectroscopy where a thin sample interacts with the standing wave formed in a Fabry-Perot cavity [70]. (b) Coherent counterpropagating waves of the same linear polarization form a standing wave of alternating electric and magnetic field anti-nodes that are sensitive to different multipole resonances[72]. (c) The electric dipole resonance of a plasmonic slot aperture metamaterial can be detected at the electric field anti-node, but not at the magnetic field anti-node (E node)[73]. (d) The magnetic dipole and electric quadrupole resonance of stacked plasmonic wires can be detected at the magnetic field anti-node, but not at the electric field anti-node (B node)[73].

In particular, co-polarized, counter-propagating, coherent linearly polarized waves form a standing wave of alternating electric and magnetic field nodes and anti-nodes, see Fig. 7b. As electric field anti-nodes correspond to magnetic field nodes, and vice versa, this allows selective material excitation with linearly polarized electric or magnetic field only, or with any ratio of electric and magnetic field strengths. In terms of multipole excitations, this enables the selective detection of even parity multipole resonances (e.g. electric dipole) of a sufficiently thin sample placed at an electric field anti-node and detection of odd parity multipole resonances (e.g. magnetic dipole and electric quadrupole) at magnetic field anti-nodes[72]. Such excitation-selective spectroscopy in standing waves has been demonstrated experimentally by Fang et al[73] using thin

plasmonic metamaterials. The electric dipole resonance of an array of slots in a single plasmonic metal layer was clearly visible for electric field excitation but could not be detected with magnetic excitation (Fig. 7c). In contrast, the magnetic dipole and electric quadrupole resonance of plasmonic wire pairs could only be detected with magnetic excitation of the nanostructure (Fig. 7d).

Selective excitation of thin films with either electric or magnetic fields as discussed above was achieved with one type of energy standing wave, which is part of a much bigger family of electromagnetic energy and polarization standing waves[74] promising further spectroscopic opportunities. Energy standing waves can be formed by counterpropagating coherent waves of parallel linear polarization or opposite circular polarizations and they are characterized by spatially oscillating electric and magnetic energy densities. Polarization standing waves are formed by counterpropagating coherent waves of orthogonal linear polarization or identical circular polarization and they are characterized by a spatially oscillating local polarization state.

Data and image processing with coherent metadevices

The signal processing opportunities presented by coherent interaction of light with light on 2D matter in a four-port device as discussed above have been investigated in detail in a theoretical study by Fang et al[75] followed by recent experimental demonstrations [76-78]. They include transistor-like small-signal amplification as well as logical operations NOT, XOR, XNOR on phase-modulated data and NOT, XOR, AND, OR on intensity-modulated data, promising fast and low energy information processing in novel coherent data processing architectures and locally coherent networks that are becoming part of the mainstream telecommunications agenda. With 100 THz bandwidth[47] and compatibility with single photon signals[48] (see next section), coherent control of light with light on 2D matter may therefore provide answers to bandwidth and energy challenges of our information society.

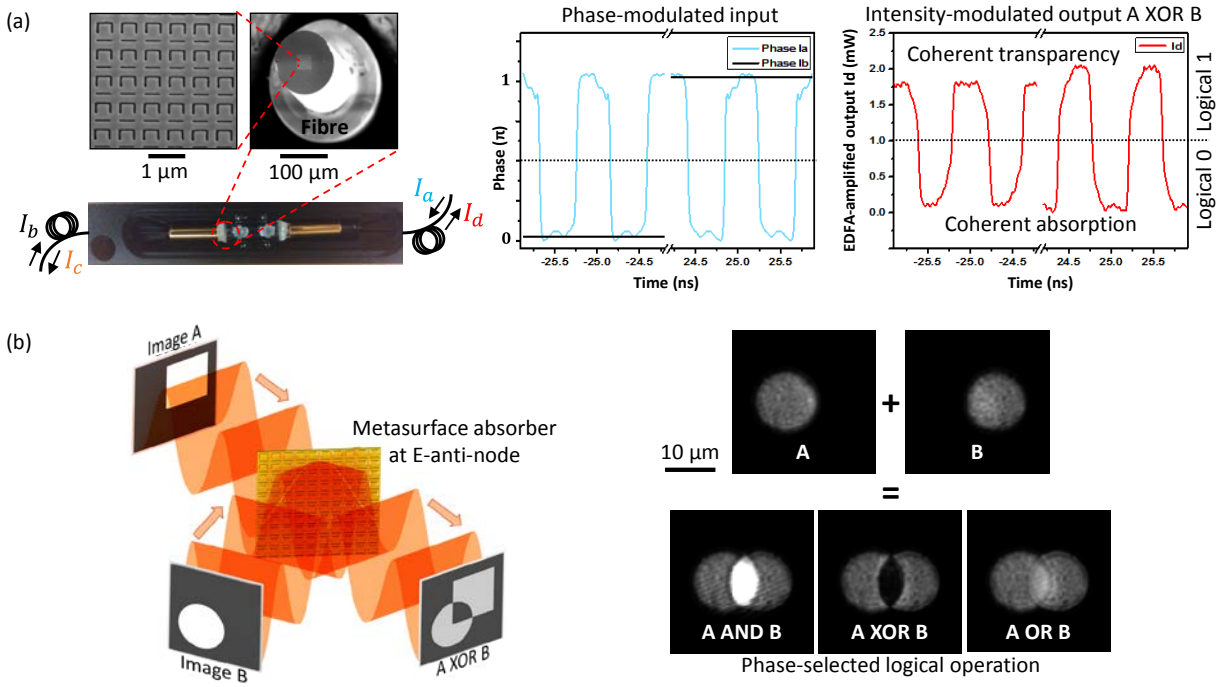

Fig. 8: Coherent data and image processing. (a) Fiberized coherent data processing metadevice consisting of a gold metasurface absorber fabricated on the cleaved end of an optical fibre. Phase-modulated input signals I_a and I_b interact on the metasurface such that identical bits are absorbed and opposite bits are transmitted, yielding an output signal I_d corresponding to an intensity-modulated signal A XOR B with a modulation rate of 1.2 GHz[76]. (b) Logical operations between images, A and B, based on projection of different images onto a metasurface absorber using coherent light. The optical phase difference in areas of image overlap controls absorption from coherent perfect transparency to coherent perfect absorption and may be set to realize logical operations A AND B, A XOR B and A OR B between the images[77].

Recently, a first fiberized coherent data processing metadevice has been demonstrated[76], see Fig. 8a. It consists of a plasmonic metasurface absorber fabricated on the core area of a cleaved optical fibre coupled to a second optical fibre by a pair of microcollimator lenses. The fully packaged four-port metadevice connects directly to standard telecoms fibres. It exhibits the effective nonlinearity introduced by Fig. 3 as well as several logical functions. For example, an XOR operation on binary phase-modulated data, where logical states of "1" and "0" are represented by equal intensity and opposite phase is shown by Fig. 8a. The XOR operation between input signals A and B results from absorption of identical bits due to constructive interference on the metasurface absorber and transmission of opposite bits due to destructive interference on the metasurface, yielding an intensity-modulated output signal A XOR B that has been demonstrated at modulation frequencies of up to 1.2 GHz. Other signal processing functions such as signal inversion have been demonstrated at effective bitrates of up to 40 Gbit/s.

In contrast to electronics, where every signal requires a separate wire, massively parallel information processing is easily realized in optics, where imaging systems transmit essentially separate information channels spaced by the diffraction limit. Therefore, "zero-dimensional" coherent control of one beam of light with another, as considered above, may be extended to "two-dimensional" coherent control of light with light by projecting different images onto opposite sides of a metasurface absorber using coherent light, see Fig. 8b. This has been demonstrated by Papaioannou et al[77] for the simplest possible case of imaging two misaligned apertures onto a metasurface absorber. In the regions of image overlap, the phase difference between the illuminating light beams controls absorption of light by the metasurface. Destructive interference in areas of image overlap highlights the similarities of images A and B due to coherent perfect transparency and therefore yields an output image A AND B. On the other hand, constructive interference deletes the similarities by coherent absorption, leaving only the image differences and therefore yields an output image A XOR B. The phase-dependent power fluctuation of the output image is therefore proportional to the area of image overlap, while the minimum power contained in the output image is a measure of the image differences, enabling pattern recognition and image analysis applications[79]. Further importance is derived from the exponential growth of telecommunications bandwidth that will require information transfer in multiple spatial information channels, e.g. in multi-core optical fibres. Here, two-dimensional control of light with light can provide solutions for both ultrafast parallel data processing as well as selection and deletion of selected information channels[78].

However, despite demonstrations of various single-channel and multi-channel signal processing operations, there are still significant challenges that need to be overcome before complex coherent information processing systems can become a reality[80], for example relating to phase stability and cascading of multiple signal processing steps. The phase stability that will be required across the entire system may be achieved by miniaturization and a monolithic platform that could be based on silicon photonics. Cascading of coherent signal processing steps will require the output of one coherent interaction to be a suitable input for the next, implying that signal regeneration may be needed in between signal processing steps to avoid accumulation of noise.

Coherent absorption of light in the quantum regime

Conventional modulation of light with light based on optical nonlinearities is strongly intensity-dependent and requires a minimum level of intensity to activate the nonlinear response. In contrast, coherent control of light with light as discussed above is linear in the sense that equal scaling of all coherent signals incident on a 2D material will result in scaling of all output signals by the same factor. Recently, it has been demonstrated that this remains true at arbitrarily low intensities and even in the single photon regime[48], unlocking interesting and counterintuitive opportunities for deterministic control of single as well as entangled quanta of light.

Historically, losses and dissipation have typically been considered highly undesirable in the field of quantum optics[81] as losses occur at the expense of additional fluctuations and noise in the system[82-83]. It was therefore generally thought that dissipation should at all costs be minimised or avoided. However, recent advances in the field of quantum plasmonics[84] have paved the way to the study of quantum effects in the context of coherent perfect absorption. While absorption of photons from a travelling wave is probabilistic, coherent perfect absorption can be observed deterministically even with a single photon, which may be coupled into a localized plasmon with nearly 100% probability[48]. Also, two-photon N00N states can be commanded to exclusively exhibit either single- or two-photon absorption[85]. A counterintuitive and currently debated possibility is that dissipation can actually lengthen the coherence time of a certain subsystem thus possibly

even providing a route for the observation of quantum effects in "warm" environments such as photosynthesis or other biological systems[86-88].

More specifically to the control of photon states, the presence of loss, if properly harnessed, can be used as a resource that can shape the specific output modes from a beamsplitter in ways that are not achievable without loss. The first theoretical studies in this sense were carried out by Barnett and co-workers who analysed the behaviour of a lossy beamsplitter inserted in a Hong-Ou-Mandel interferometer[89].

Hong-Ou-Mandel interference is a quantum effect whereby two photons simultaneously entering two ports of a beam splitter will be forced to bunch together, i.e. they can exit from either output port, but both photons must exit from the same port[90]. It is not possible to know which output port the two photons will bunch into. Therefore, two photons interfering at the beamsplitter will create what is known as a N00N state at the beamsplitter output. A N00N state is an entangled state and is so-called after the bra-ket notation used to describe the situation in which 2 photons (or N photons) are in a superposition state of being either N in one arm or N in the other arm of an interferometer. Such path-entangled states can be used as a resource for quantum metrology as they can provide an *N*-fold enhancement in interferometer-based phase measurements. N00N states from photon bunching at a beamsplitter are generally obtained with a lossless beamsplitter. The more general case in which loss occurs at the beamsplitter leads to more complicated output states. Without going into the details of the most general case studied by Barnett et al.[89], we will consider the specific situation in which absorption is equal to exactly 50% in a very thin film (compared to the wavelength of the photon). For the simplest case of a single photon input state (*N*=1) with appropriate phases, the single photon is either deterministically absorbed or completely transmitted, thus providing a "lossless lossy beamsplitter"[91]. This of course is just a quantum restatement of coherent perfect absorption for a single photon[92]. Coherent perfect absorption of a single photon was verified experimentally by Roger et al. thus extending coherent perfect absorption into the single photon regime[48]. For appropriate two-photon input states (*N*=2), the lossy beam splitter can yield deterministic absorption of a single photon as well as situations where the two photons must be either both transmitted or both absorbed. The latter is reminiscent of nonlinear absorption processes although it is important to recall that the "linear" two-photon absorption described here requires linear absorption at the input wavelength of the two input photons (in contrast to nonlinear two-photon absorption that can occur in a medium that is transparent at the input wavelength). Thus, quantum states in the regime of coherent perfect absorption can lead to rather unexpected output states and situations such as linear two-photon absorption that do not have a direct analogue in classical optics. The first experimental verification of coherent perfect absorption with two-photon N00N states was performed by Roger et al. and was carried out using a multilayer graphene beamsplitter[85]. By tailoring the number of layers (2.3% absorption per layer), it is possible to achieve close to ideal 50% absorption in a graphene film of several nm thickness deposited on a glass substrate that is then used as the lossy beamsplitter. The input states are generated in a Hong-Ou-Mandel interferometer that is in turn illuminated with photon pairs obtained by parametric down-conversion in a BBO crystal. The output of the Hong-Ou-Mandel interferometer is fed into a Sagnac-interferometer, similar to that used for classical coherent perfect absorption measurements. The output states are then measured by extracting 50% of the photons with beamsplitters placed on either side of the lossy film. In such a way it was indeed possible to verify that by changing the phase of the input states, the total photon counts oscillate, thus providing indirect evidence of the oscillation between single and two-photon absorption.

The extra degree of freedom offered by loss can also be used to achieve other forms of coherent control of quantum states. For example, Vest et al, showed that loss can lead to anti-bunching of bosons in a Hong-Ou-Mandel interferometer[93], i.e. the Hong-Ou-Mandel interferometer "dip" is replaced by a "peak". This fermionic anticoalescence of photons at a beamsplitter, here obtained as a result of dissipation at the beamsplitter, had only been observed before by purposely shaping the input photons so that their wavefunctions where antisymmetric. Here, the common notion of boson bunching on a dielectric beamsplitter is overturned by resorting to the unique degree of freedom offered by lossy beamsplitters in tailoring the exact phase relation between reflection and transmission.

As a last example of progress in the field, we highlight recent work that extends previous quantum eraser experiments to include coherent perfect absorption[94]. If we consider the simple case of single photon interference, this may be inhibited by providing which-path information in the interferometer (e.g. by polarization rotation with a wave plate in one arm). During the post-measurement process, it is however possible to "erase" the information by post-selecting data based on measurements performed on a nonlocal detector[95-96]. The erasure scheme is enabled by entanglement of the photon inside the interferometer and

the “control” photon, detected outside (nonlocally to) the interferometer. In the experiment by Altuzarra et al., a single photon is sent into a coherent perfect absorption interferometer such as that shown in Fig. 9. The photon is one of a pair of polarisation entangled photons: for example, the polarisation of an individual photon is either vertical or horizontal but is not pre-determined in a single measurement. However, measurement of the polarisation of one photon fixes the polarisation of the other to be opposite. Which-path information is introduced by a half-wave plate oriented at 45° inside only one arm of the interferometer: H-polarised photons travelling in that arm will be rotated to V and vice versa. Therefore, measurements performed on the single photon in the interferometer do not reveal any coherent perfect absorption effects due to the fact that the counterpropagating photon mode functions are oppositely polarised and can no longer form an energy standing wave. However, polarisation sensitive measurements on the second (nonlocal) photon, allow to immediately establish the polarisation of the other photon: by post-selecting all measurements corresponding to a fixed polarisation of $\pm 45°$ at the nonlocal detector, one fixes the polarisation to $\mp 45°$ in the interferometer (that is not modified by the half-wave plate): which-path information is erased and coherent perfect absorption interference fringes are now observed. The quantum nature of this process is also directly verified by reducing the degree of entanglement of the two input photons and thus observing a corresponding decrease in the coherent perfect absorption visibility[94].

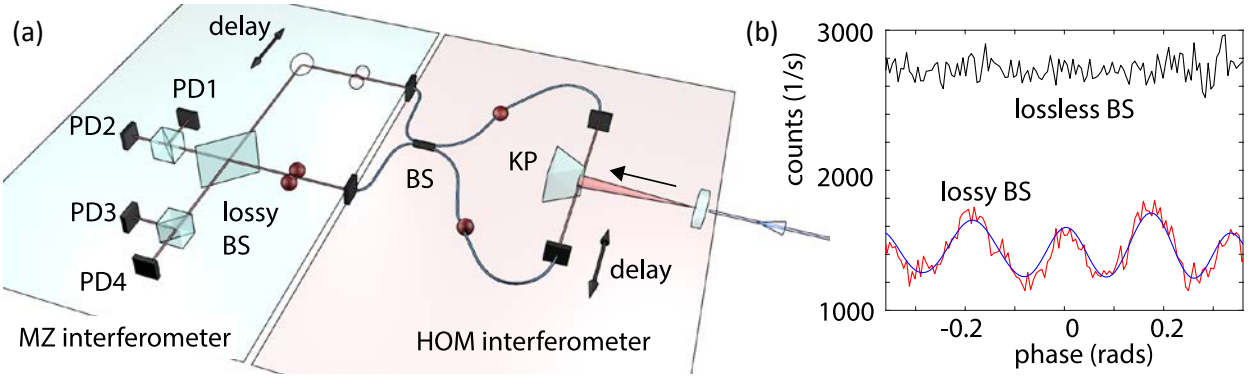

Fig. 9: Coherent absorption in the quantum regime. (a) Experimental layout used to measure coherent perfect absorption with entangled N00N states. Photon pairs generated in a BBO crystal are filtered and split at a knife edge prism (KP). They are then coupled into the Hong-Ou-Mandel interferometer with single mode fibres and directed to a 50/50 beamsplitter (BS). A delay stage ensures the photons arrive at the same time on the beamsplitter and hence bunch, forming a N00N state. The *N*=2 N00N state is directed into a Sagnac or, in this case, a Mach-Zehnder (MZ) interferometer. The N00N state interferes with itself on the lossy beam splitter and the output states are characterised by a series of four photon detectors (PD) and beamsplitters. (b) By scanning the N00N state phase with a delay stage, oscillations are seen in the total output coincidence counts. These correspond to the output state oscillating between a mixed state and a pure entangled N00N state with one photon less (*N*=1). The black line shows the same measurement performed with a lossless beamsplitter: no oscillations in the coincidence counts are observed, reflecting the fact that the photon number is conserved.

This brief overview of recent results shows how absorption is gaining recognition as a resource in quantum optics and as such, coherent control of absorption presents new opportunities for both fundamental studies and applications alike, enriching the quantum toolbox.

Summary

Control of light with light used to be the domain of nonlinear optics, however, the coherent interaction of light with light on linear planar functional (meta)materials has enabled control over a huge range of optical phenomena. Instead of relying on optically nonlinear materials, dynamic control of light with light is derived from the fact that the interference of two coherent beams of light controls the local field that interacts with the linear planar material. This allows the manifestation of the film’s optical functionalities to be controlled from complete suppression by destructive interference to enhancement by constructive interference. In contrast to optical nonlinearities, such coherent control of light with light offers high contrast and 100 THz bandwidth at arbitrary intensities down to the single photon quantum regime. Therefore, this approach offers

a broad range of opportunities for all-optical signal and image processing as well as quantum technologies. In addition, interference of coherent light fields allows selective probing of thin films with either electric or magnetic fields, opening up novel opportunities for spectroscopy.

Author Information

Corresponding authors

E-mail: erp@orc.soton.ac.uk; kfm@orc.soton.ac.uk; niz@orc.soton.ac.uk

Notes

The authors declare no competing financial interests.

Acknowledgement

The authors thank Jianfa Zhang, Maria Papaioannou, Angelos Xomalis, Yidong Chong and Robert Boyd for fruitful discussions. This work is supported by the UK's Engineering and Physical Sciences Research Council (grant EP/M009122/1) and the MOE Singapore (grant MOE2011-T3-1-005). No new data were created as part of this review.

References

1. Shapiro M, B. P., *Principles of the Quantum Control of Molecular Processes*. John Wiley & Sons Inc.: New York, 2003.
2. Reiter, D. E.; Sherman, E. Y.; Najmaie, A.; Sipe, J. E., Coherent control of electron propagation and capture in semiconductor heterostructures. *Europhys. Lett.* **2009,** *88* (6), 67005.
3. A. Assion, T. B., M. Bergt, T. Brixner, B. Kiefer, V. Seyfried, M. Strehle, G. Gerber, Control of Chemical Reactions by Feedback-Optimized Phase-Shaped Femtosecond Laser Pulses. *Science* **1998,** *282* (5390), 919-922.
4. Chong, Y. D.; Ge, L.; Cao, H.; Stone, A. D., Coherent Perfect Absorbers: Time-Reversed Lasers. *Phys. Rev. Lett.* **2010,** *105*, 053901.
5. Wan, W.; Chong, Y.; Ge, L.; Noh, H.; Stone, A. D.; Cao, H., Time-Reversed Lasing and Interferometric Control of Absorption. *Science* **2011,** *331*, 889-892.
6. Yoon, J. W.; Koh, G. M.; Song, S. H.; Magnusson, R., Measurement and Modeling of a Complete Optical Absorption and Scattering by Coherent Surface Plasmon-Polariton Excitation Using a Silver Thin-Film Grating. *Phys. Rev. Lett.* **2012,** *109*, 257402.
7. Noh, H.; Chong, Y.; Stone, A. D.; Cao, H., Perfect coupling of light to surface plasmons by coherent absorption. *Phys. Rev. Lett.* **2012,** *108*, 186805.
8. Pye, L. N.; Villinger, M. L.; Shabahang, S.; Larson, W. D.; Martin, L.; Abouraddy, A. F., Octave-spanning coherent perfect absorption in a thin silicon film. *Opt. Lett.* **2017,** *42* (1), 151-154.
9. Stockman, M. I.; Faleev, S. V.; Bergman, D. J., Coherent Control of Femtosecond Energy Localization in Nanosystems. *Phys. Rev. Lett.* **2002,** *88*, 067402.
10. Li, X.; Stockman, M. I., Highly efficient spatiotemporal coherent control in nanoplasmonics on a nanometer-femtosecond scale by time reversal. *Phys. Rev. B* **2008,** *77*, 195109.
11. Kao, T. S.; Jenkins, S. D.; Ruostekoski, J.; Zheludev, N. I., Coherent Control of Nanoscale Light Localization in Metamaterial: Creating and Positioning Isolated Subwavelength Energy Hot Spots. *Phys. Rev. Lett.* **2011,** *106*, 085501.
12. Gjonaj, B.; Aulbach, J.; Johnson, P. M.; Mosk, A. P.; Kuipers, L.; Lagendijk, A., Active spatial control of plasmonic fields. *Nat. Photonics* **2011,** *5*, 360-363.
13. Brinks, D.; Castro-Lopez, M.; Hildner, R.; van Hulst, N. F., Plasmonic antennas as design elements for coherent ultrafast nanophotonics. *Proc. Natl. Acad. Sci. U.S.A.* **2013,** *110*, 18386–18390.
14. Scalora, M.; Bloemer, M. J.; Pethel, A. S.; Dowling, J. P.; Bowden, C. M.; Manka, A. S., Transparent, metallo-dielectric, one-dimensional, photonic band-gap structures. *J. Appl. Phys.* **1998,** *83* (5), 2377-2383.
15. Scalora, M.; Bloemer, M. J.; Bowden, C. M., Metals under a new light. *Opt Photonics News* **1999,** *10* (9), 25-27.

16. Bruck, R.; Muskens, O. L., Plasmonic nanoantennas as integrated coherent perfect absorbers on SOI waveguides for modulators and all-optical switches. *Opt. Express* **2013,** *21* (23), 27662-71.
17. Park, H.; Lee, S. Y.; Kim, J.; Lee, B.; Kim, H., Near-infrared coherent perfect absorption in plasmonic metal-insulator-metal waveguide. *Opt. Express* **2015,** *23* (19), 24464-74.
18. Rothenberg, J. M.; Chen, C. P.; Ackert, J. J.; Dadap, J. I.; Knights, A. P.; Bergman, K.; Osgood, R. M.; Grote, R. R., Experimental demonstration of coherent perfect absorption in a silicon photonic racetrack resonator. *Opt. Lett.* **2016,** *41* (11), 2537-40.
19. Utikal, T.; Stockman, M. I.; Heberle, A. P.; Lippitz, M.; Giessen, H., All-Optical Control of the Ultrafast Dynamics of a Hybrid Plasmonic System. *Phys. Rev. Lett.* **2010,** *104*, 113903.
20. Papoff, F.; McArthur, D.; Hourahine, B., Coherent control of radiation patterns of nonlinear multiphoton processes in nanoparticles. *Sci. Rep.* **2015,** *5*, 12040.
21. Crescimanno, M.; Dawson, N. J.; Andrews, J. H., Coherent perfect rotation. *Phys. Rev. A* **2012,** *86*, 031807(R).
22. Crescimanno, M.; Zhou, C.; Andrews, J. H.; Baker, M. A., Structure and symmetry in coherent perfect polarization rotation. *Phys. Rev. A* **2015,** *91* (1).
23. Friedrich, D.; Kaufer, H.; Westphal, T.; Yamamoto, K.; Sawadsky, A.; Khalili, F. Y.; Danilishin, S. L.; Goßler, S.; Danzmann, K.; Schnabel, R., Laser interferometry with translucent and absorbing mechanical oscillators. *New J. Phys.* **2011,** *13*, 093017.
24. Yan, X. B.; Cui, C. L.; Gu, K. H.; Tian, X. D.; Fu, C. B.; Wu, J. H., Coherent perfect absorption, transmission, and synthesis in a double-cavity optomechanical system. *Opt. Express* **2014,** *22* (5), 4886-4895.
25. Choi, S. B.; Park, D. J.; Jeong, Y. K.; Yun, Y. C.; Jeong, M. S.; Byeon, C. C.; Kang, J. H.; Park, Q. H.; Kim, D. S., Directional control of surface plasmon polariton waves propagating through an asymmetric Bragg resonator. *Appl. Phys. Lett.* **2009,** *94*, 063115.
26. Li, Z.; Zhang, S.; Halas, N. J.; Nordlander, P.; Xu, H., Coherent Modulation of Propagating Plasmons in Silver-Nanowire-Based Structures. *Small* **2011,** *7*, 593–596.
27. Miyata, M.; Takahara, J., Excitation control of long-range surface plasmons by two incident beams. *Opt. Express* **2012,** *20*, 9493-9500.
28. Wei, P.; Croënne, C.; Tak Chu, S.; Li, J., Symmetrical and anti-symmetrical coherent perfect absorption for acoustic waves. *Appl. Phys. Lett.* **2014,** *104* (12), 121902.
29. Meng, C.; Zhang, X.; Tang, S. T.; Yang, M.; Yang, Z., Acoustic Coherent Perfect Absorbers as Sensitive Null Detectors. *Sci. Rep.* **2017,** *7*, 43574.
30. Pozar, D. M., *Microwave engineering*. 2 ed.; John Wiley & Sons Inc.: 1998.
31. Jackson, J. D., *Classical Electrodynamics*. 3 ed.; John Wiley & Sons: New York, 1998.
32. Troitskii, Y. V., Optical resonator with a thin absorbing film as a mode selector. *Opt. Spectrosc.* **1968,** *25*, 309-313.
33. Troitskii, Y. V.; Goldina, N. D., Separation of one mode in a laser. *JETP Lett.* **1968,** *7*, 36.
34. Smith, P. W.; Schneider, M. V.; Danielmeyer, H. G., High-Power Single-Frequency Lasers Using Thin Metal Film Mode-Selection Filters. *Bell Syst. Tech. J.* **1969,** *48*, 1405
35. Avtonomov, V. P.; Antropov, E. T.; Sobolev, N. N.; Troitskii, Y. V., Separation of rotational lines of a CO2 laser with a film selector in the resonator. *Sov. J. Quantum Electron.* **1972,** *2* (3), 300-302.
36. Miller, A. B., Laser tuners and wavelength-selective detectors based on absorbers in standing waves. *IEEE J. of Quantum Electron.* **1994,** *30* (3), 732-749.
37. Babin, S. A.; Kablukov, S. I.; Terentiev, V. S., Reflection interferometer based on the Troitsky thin film for frequency selection in fiber lasers. *Laser Phys.* **2008,** *18* (11), 1241-1245.
38. Hägglund, C.; Apell, S. P.; Kasemo, B., Maximized Optical Absorption in Ultrathin Films and Its Application to Plasmon-Based Two-Dimensional Photovoltaics. *Nano Lett.* **2010,** *10*, 3135-3141.
39. Thongrattanasiri, S.; Koppens, F. H. L.; García de Abajo, F. J., Complete Optical Absorption in Periodically Patterned Graphene. *Phys. Rev. Lett.* **2012,** *108*, 047401.
40. Zhang, J.; MacDonald, K. F.; Zheludev, N. I., Controlling light-with-light without nonlinearity. *Light Sci. Appl.* **2012,** *1*, e18.
41. Dutta-Gupta, S.; Martin, O. J. F.; Dutta Gupta, S.; Agarwal, G. S., Controllable coherent perfect absorption in a composite film. *Opt. Express* **2012,** *20*, 1330-1336.

42. Yu, S.; Piao, X.; Hong, J.; Park, N., Progress toward high-Qperfect absorption: A Fano antilaser. *Phys. Rev. A* **2015,** *92* (1).
43. Wong, Z. J.; Xu, Y.-L.; Kim, J.; O'Brien, K.; Wang, Y.; Feng, L.; Zhang, X., Lasing and anti-lasing in a single cavity. *Nat. Photonics* **2016,** *10* (12), 796-801.
44. Zheludev, N. I.; Kivshar, Y. S., From metamaterials to metadevices. *Nat. Mater.* **2012,** *11*, 917-924.
45. Plum, E.; Tanaka, K.; Chen, W. T.; Fedotov, V. A.; Tsai, D. P.; Zheludev, N. I., A combinatorial approach to metamaterials discovery. *J. Opt.* **2011,** *13*, 055102.
46. Fang, X.; Tseng, M. L.; Ou, J. Y.; MacDonald, K. F.; Tsai, D. P.; Zheludev, N. I., Ultrafast all-optical switching via coherent modulation of metamaterial absorption. *Appl. Phys. Lett.* **2014,** *104*, 141102.
47. Nalla, V.; Valente, J.; Sun, H.; Zheludev, N. I., 11-fs dark pluses generated via coherent absorption in plasmonic metamaterial. *Opt. Express* **2017,** *25* (19), 22620 - 22625.
48. Roger, T.; Vezzoli, S.; Bolduc, E.; Valente, J.; Heitz, J. J. F.; Jeffers, J.; Soci, C.; Leach, J.; Couteau, C.; Zheludev, N. I.; Faccio, D., Coherent perfect absorption in deeply subwavelength films in the single-photon regime. *Nat. Commun.* **2015,** *6*, 7031.
49. Nalla, V.; Karvounis, A.; Valente, J.; Sun, H. D.; Zheludev, N. I., Ultrafast Regimes of Coherent Absorption in Plasmonic and Dielectric Diamond-based Metasurfaces. In *ICMAT2017*, Singapore, 2017.
50. Fan, Y.; Liu, Z.; Zhang, F.; Zhao, Q.; Wei, Z.; Fu, Q.; Li, J.; Gu, C.; Li, H., Tunable mid-infrared coherent perfect absorption in a graphene meta-surface. *Sci. Rep.* **2015,** *5*, 13956.
51. Nie, G.; Shi, Q.; Zhu, Z.; Shi, J., Selective coherent perfect absorption in metamaterials. *Appl. Phys. Lett.* **2014,** *105*, 201909.
52. Pu, M.; Feng, Q.; Wang, M.; Hu, C.; Huang, C.; Ma, X.; Zhao, Z.; Wang, C.; Luo, X., Ultrathin broadband nearly perfect absorber with symmetrical coherent illumination. *Opt. Express* **2012,** *20*, 2246-2254.
53. Rao, S. M.; Heitz, J. J. F.; Roger, T.; Westerberg, N.; Faccio, D., Coherent control of light interaction with graphene. *Opt. Lett.* **2014,** *39* (18), 5345-5374.
54. Boyd, R. W., *Nonlinear Optics*. 3rd ed. ed.; Academic Press: San Diego, CA, USA, 2008.
55. Shi, J.; Fang, X.; Rogers, E. T. F.; Plum, E.; MacDonald, K. F.; Zheludev, N. I., Coherent control of Snell's law at metasurfaces. *Opt. Express* **2014,** *22* (17), 21051-21060.
56. Yu, N.; Genevet, P.; Kats, M. A.; Aieta, F.; Tetienne, J.-P.; Capasso, F.; Gaburro, Z., Light Propagation with Phase Discontinuities: Generalized Laws of Reflection and Refraction. *Science* **2011,** *334* (6054), 333-337.
57. Kita, S.; Takata, K.; Ono, M.; Nozaki, K.; Kuramochi, E.; Takeda, K.; Notomi, M., Coherent control of high efficiency metasurface beam deflectors with a back partial reflector. *APL Photonics* **2017,** *2* (4), 046104.
58. Ni, X.; Ishii, S.; Kildishev, A. V.; Shalaev, V. M., Ultra-thin, planar, Babinet-inverted plasmonic metalenses. *Light Sci. Appl.* **2013,** *2* (4), e72.
59. Chen, X.; Huang, L.; Muhlenbernd, H.; Li, G.; Bai, B.; Tan, Q.; Jin, G.; Qiu, C. W.; Zhang, S.; Zentgraf, T., Dual-polarity plasmonic metalens for visible light. *Nat. Commun.* **2012,** *3*, 1198.
60. Ni, X.; Kildishev, A. V.; Shalaev, V. M., Metasurface holograms for visible light. *Nat. Commun.* **2013,** *4*.
61. Huang, L.; Chen, X.; Mühlenbernd, H.; Zhang, H.; Chen, S.; Bai, B.; Tan, Q.; Jin, G.; Cheah, K.-W.; Qiu, C.-W.; Li, J.; Zentgraf, T.; Zhang, S., Three-dimensional optical holography using a plasmonic metasurface. *Nat. Commun.* **2013,** *4*.
62. Mousavi, S. A.; Plum, E.; Shi, J.; Zheludev, N. I., Coherent control of birefringence and optical activity. *Appl. Phys. Lett.* **2014,** *105*, 011906.
63. Plum, E.; Liu, X. X.; Fedotov, V. A.; Chen, Y.; Tsai, D. P.; Zheludev, N. I., Metamaterials: optical activity without chirality. *Phys. Rev. Lett.* **2009,** *102* (11), 113902.
64. Mousavi, S. A.; Plum, E.; Shi, J.; Zheludev, N. I., Coherent control of optical polarization effects in metamaterials. *Sci. Rep.* **2015,** *5*, 8977.
65. Hiramatsu, K.; Plum, E.; Valente, J.; MacDonald, K. F.; Zheludev, N. I. In *Coherent Spectroscopy of Optical Activity*, CLEO/Europe-EQEC 2015, Munich, Germany, 21-25 June 2015; Munich, Germany, 2015.

66. Pirruccio, G.; Ramezani, M.; Rodriguez, S. R.; Rivas, J. G., Coherent Control of the Optical Absorption in a Plasmonic Lattice Coupled to a Luminescent Layer. *Phys. Rev. Lett.* **2016,** *116* (10), 103002.
67. Rao, S. M.; Lyons, A.; Roger, T.; Clerici, M.; Zheludev, N. I.; Faccio, D., Geometries for the coherent control of four-wave mixing in graphene multilayers. *Sci. Rep.* **2015,** *5*, 15399.
68. Pirruccio, G.; Rivas, J. G., Modulated light absorption and emission of a luminescent layer by phase-controlled multiple beam illumination. *Opt. Express* **2015,** *23* (14), 18166-80.
69. Terasaki, A.; Kondow, T.; Egashira, K., Continuous-wave cavity ringdown spectroscopy applied to solids: properties of a Fabry-Perot cavity containing a transparent substrate. *J. Opt. Soc. Am. B* **2005,** *22* (3), 675-686.
70. Egashira, K.; Terasaki, A.; Kondow, T., Photon-trap spectroscopy applied to molecules adsorbed on a solid surface: probing with a standing wave versus a propagating wave. *Appl. Opt.* **2010,** *49* (7), 1151-1157.
71. Wei, L.; Xi, Z.; Bhattacharya, N.; Urbach, H. P., Excitation of the radiationless anapole mode. *Optica* **2016,** *3* (8), 799.
72. Tseng, M. L.; Fang, X.; Savinov, V.; Wu, P. C.; Ou, J. Y.; Zheludev, N. I.; Tsai, D. P., Coherent selection of invisible high-order electromagnetic excitations. *Sci. Rep.* **2017,** *7*, 44488.
73. Fang, X.; Tseng, M. L.; Tsai, D. P.; Zheludev, N. I., Coherent Excitation-Selective Spectroscopy of Multipole Resonances. *Phys. Rev. Appl.* **2016,** *5*, 014010.
74. Fang, X.; MacDonald, K. F.; Plum, E.; Zheludev, N. I., Coherent control of light-matter interactions in polarization standing waves. *Sci. Rep.* **2016,** *6*, 31141.
75. Fang, X.; MacDonald, K. F.; Zheludev, N. I., Controlling light with light using coherent metadevices: all-optical transistor, summator and invertor. *Light Sci. Appl.* **2015,** *4*, e292.
76. Xomalis, A.; Demirtzioglou, I.; Plum, E.; Jung, Y.; Nalla, V.; Lacava, C.; MacDonald, K. F.; Petropoulos, P.; Richardson, D. J.; Zheludev, N. I., Fibre-optic metadevice for all-optical signal modulation based on coherent absorption. *arXiv* **2017**, 1709.05357.
77. Papaioannou, M.; Plum, E.; Valente, J.; Rogers, E. T. F.; Zheludev, N. I., Two-dimensional control of light with light on metasurfaces. *Light Sci. Appl.* **2016,** *5*, e16070.
78. Papaioannou, M.; Plum, E.; Valente, J.; Rogers, E. T. F.; Zheludev, N. I., All-optical multichannel logic based on coherent perfect absorption in a plasmonic metamaterial. *APL Photonics* **2016,** *1*, 090801.
79. Papaioannou, M.; Plum, E.; Zheludev, N. I., All-Optical Pattern Recognition and Image Processing on a Metamaterial Beam Splitter. *ACS Photonics* **2017,** *4* (2), 217-222.
80. Miller, D. A. B., Are optical transistors the logical next step? *Nat. Photonics* **2010,** *4* (1), 3-5.
81. Walls, D. F.; Milburn, G. J., Effect of dissipation on quantum coherence. *Phys. Rev. A* **1985,** *31* (4), 2403-2408.
82. Callen, H. B.; Welton, T. A., Irreversibility and Generalized Noise. *Phys. Rev.* **1951,** *83* (1), 34-40.
83. Kubo, R., The fluctuation-dissipation theorem. *Rep. Prog. Phys.* **1966,** *29*, 255.
84. Tame, M. S.; McEnery, K. R.; Özdemir, Ş. K.; Lee, J.; Maier, S. A.; Kim, M. S., Quantum plasmonics. *Nat. Phys.* **2013,** *9* (6), 329-340.
85. Roger, T.; Restuccia, S.; Lyons, A.; Giovannini, D.; Romero, J.; Jeffers, J.; Padgett, M.; Faccio, D., Coherent Absorption of N00N States. *Phys. Rev. Lett.* **2016,** *117*, 023601.
86. Müller, M.; Diehl, S.; Pupillo, G.; Zoller, P., Engineered Open Systems and Quantum Simulations with Atoms and Ions. *Adv. At. Mol. Opt. Phy.* **2012,** *61*, 1-80.
87. Verstraete, F.; Wolf, M. M.; Ignacio Cirac, J., Quantum computation and quantum-state engineering driven by dissipation. *Nat. Phys.* **2009,** *5* (9), 633-636.
88. Barreiro, J. T.; Muller, M.; Schindler, P.; Nigg, D.; Monz, T.; Chwalla, M.; Hennrich, M.; Roos, C. F.; Zoller, P.; Blatt, R., An open-system quantum simulator with trapped ions. *Nature* **2011,** *470* (7335), 486-491.
89. Barnett, S.; Jeffers, J.; Gatti, A.; Loudon, R., Quantum optics of lossy beam splitters. *Phys. Rev. A* **1998,** *57*, 2134-2145.
90. Hong, C. K.; Ou, Z. Y.; Mandel, L., Measurement of Subpicosecond Time Intervals between Two Photons by Interference. *Phys. Rev. Lett.* **1987,** *59* (18), 2044-2046.
91. Jeffers, J., Interference and the lossless lossy beam splitter. *J. Mod. Opt.* **2000,** *47*, 10.

92. Huang, S.; Agarwal, G. S., Coherent perfect absorption of path entangled single photons. *Opt. Express* **2014,** *22* (17), 20936.
93. Vest, B.; Dheur, M.-C.; Devaux, É.; Baron, A.; Rousseau, E.; Hugonin, J.-P.; Greffet, J.-J.; Messin, G.; Marquier, F., Anti-coalescence of bosons on a lossy beam splitter. *Science* **2017**, in press.
94. Altuzarra, C. M. X.; Vezzoli, S.; Valente, J.; Gao, W.; Soci, C.; Faccio, D.; Couteau, C., Coherent perfect absorption in metamaterials with entangled photons. *ACS Photonics* **2017**, in press.
95. Scully, M. O.; Drühl, K., Quantum eraser: A proposed photon correlation experiment concerning observation and "delayed choice" in quantum mechanics. *Phys. Rev. A* **1982,** *25* (4), 2208-2213.
96. Walborn, S. P.; Terra Cunha, M. O.; Pádua, S.; Monken, C. H., Double-slit quantum eraser. *Phys. Rev. A* **2002,** *65* (3).

For Table of Contents Use Only

Title: Controlling the optical response of 2d matter in standing waves

Authors: Eric Plum, Kevin F. MacDonald, Xu Fang, Daniele Faccio, Nikolay I. Zheludev

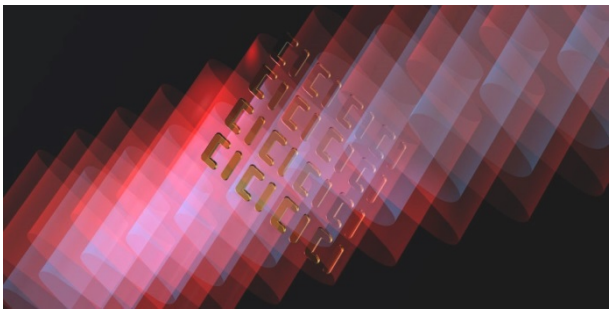

Image description:

Artistic impression of a metasurface interacting with an optical standing wave. Image created by Phil Saunders Graphics.